Chin. J. Astron. Astrophys. Vol. 2 (2002), No. 1, 33–42
(*http://www.chjaa.org* or *http://chjaa.bao.ac.cn*)

Chinese Journal of Astronomy and Astrophysics

A Study of the Energy Sources of Herbig-Haro Objects

Jing-Wen Wu, Yue-Fang Wu ⋆, Jun-Zhi Wang and Kai Cai

Department of Astronomy, CAS-PKU Joint Beijing Astrophysics Center, Peking University, Beijing 100871

Received 2001 June 25 ; accepted 2001 August 28

Abstract We make a statistical study of the energy sources of high-velocity phenomena, Herbig-Haro (HH) objects. IRAS counterparts of HH objects are identified. Their colors, brightness, geometric relation to the HH objects and SED are analysed. The sources are found to be concentrated in a band-shaped region in the IRAS color-color diagram. We suggest an explanation of thick surrounding material for this distribution. We propose a new method for identifying the energy sources based on color and brightness. This method is applied to more than 200 HH objects whose energy sources are still unknown. Finally, a group of very young stellar object candidates which have similar properties to the HH energy sources is picked out. Their large-scale distribution is discussed.

Key words: star: formation – ISM: Herbig-Haro objects – stars: pre-main-sequence

1 INTRODUCTION

Herbig-Haro objects are a kind of semi-star, semi-nebula objects associated with star forming regions. Although such objects were noticed by Burnham as early as 1890s, they did not attract much attention until the late 1940s until their independent rediscovery by Herbig and Haro in NGC 1999. A few years later, these objects were named Herbig-Haro objects for the first time by Ambartsumian (Reipurth 1997). In the following half-century, the observation and theoretical research on HH objects have undergone great development, making notable contribution to the entire field of research on star formation. The latest General Catalogue of Herbig-Haro Objects (Repurth 1999) records some 500 HH objects.

There was a dispute on the essential characteristics of HH objects arisen in the middle of the 20th century. Herbig (1951) pointed out that their energy comes from the energy released by T Tauri stars during their mass ejections while Hoyle (1956) argued that the energy may come from accretion. It was even proposed that an HH object is a radiator containing stars inside (Bome 1956). It was not until some remarkable progress was made in the field of star formation that astronomers got to know the essentials of HH objects. Now it is widely accepted that "HH

⋆ E-mail: ywu@bac.pku.edu.cn

objects are small-scale shock regions intimately associated with star forming regions" (Reipurth 1999). In the shocked and cooling down regions, under proper temperature ($\sim 7000\,\mathrm{K}$) and density ($n_e \sim n \times 10^3 - n \times 10^4$) (Reipurth 1997), strong [SII], [OI] and some other special lines will be excited in gas clumps, giving rise to the semi-stellar semi-nebular appearance. Since this is a typical circumstance arising from bipolar outflow process of star formation, HH objects have become good tracers of star forming activities. Moreover, the HH object is produced at the early stage of star formation, so, compared with other star formation tracers, it has a shorter time scale and obvious characteristics in observation, which makes it a more direct and accurate tracer of the early stage of star forming activities.

To identify and study their energy sources is not only the key step to find the essence of HH objects, but also an effective way to probe the star formation process. Identifying the energy source, however, is a difficult issue. The current method is identification through geometric symmetry, bow shock direction, and proper motion. But the energy sources that can be identified with such data are limited. More cases are conjectured using multi-wavelength data such as near-infrared, Hα, 1.3 mm emission and so on. Up to now quite a number of HH objects still have their energy sources unidentified. A thorough study of the relationship between the characteristics of energy sources and young stellar objects (YSOs) is needed. To this end, a statistical study of known HH energy sources will help to reveal some characteristics of early-stage, young stellar objects, which in turn will not only help to explore the mechanism of the origin of HH objects, but also can be used to select candidates of early-stage YSOs which have similar properties to HH energy sources for further study.

In Section 2 we identify the IRAS counterparts of known HH energy sources. The brightness, colors, and other properties of the energy sources are analysed in Section 3 and 4. Based on the results obtained, we try to identify the energy sources in the other cases in Section 5. In Section 6 we pick out a group of early aged YSO candidates and discuss their large scale distribution.

2 IRAS IDENTIFICATION OF ENERGY SOURCES OF HH OBJECTS

The General Catalogue of HH objects (Reipurth 1999) lists about 140 energy sources of HH objects. These energy sources excite the majority of known HH objects. Among those 140 sources, some drive more than one HH object, some even entire HH clusters. Based on the General Catalogue (Reipurth 1999), the Catalog of Infrared Observations (Gezari et al. 1996) and a Pre-Main Sequence (PMS) Star Catalog (Weintraub 1990), we find 102 HH objects among the 140 to have IRAS counterparts. The fraction of sources with IRAS counterparts is more than 70%. In this paper, we first make a statistical study of these IRAS energy sources.

Figures 1a and 1b show the histograms of the linear distance (pc) and the angular distance (arcmin) between the HH and its IRAS energy source. We see that most HH objects are located within 0.5 pc of their energy sources and are concentrated within 0.2 pc. Nearly all the HH objects are within 10 arcmin of their energy sources.

3 PROPERTIES OF HH ENERGY SOURCES

3.1 Luminosity

The bolometric luminosities of the identified IRAS sources are calculated according to Casoli et al. (1986):

$$L_{5-1000\,\mu\mathrm{m}} = 4\pi D^2 \times 1.75 \times (F_{12}/0.79 + F_{25}/2 + F_{60}/3.9 + F_{100}/9.9)\,.$$

The frequency distribution of the IRAS luminosities of the HH energy sources is shown in Fig. 2. One can see that 80% of these sources have a $L_{5-1000\mu\mathrm{m}}$ less than $50\,L_{\odot}$. Only 11 sources has a larger luminosity than $300\,L_{\odot}$. These data suggest that the HH energy sources are primarily low-mass objects.

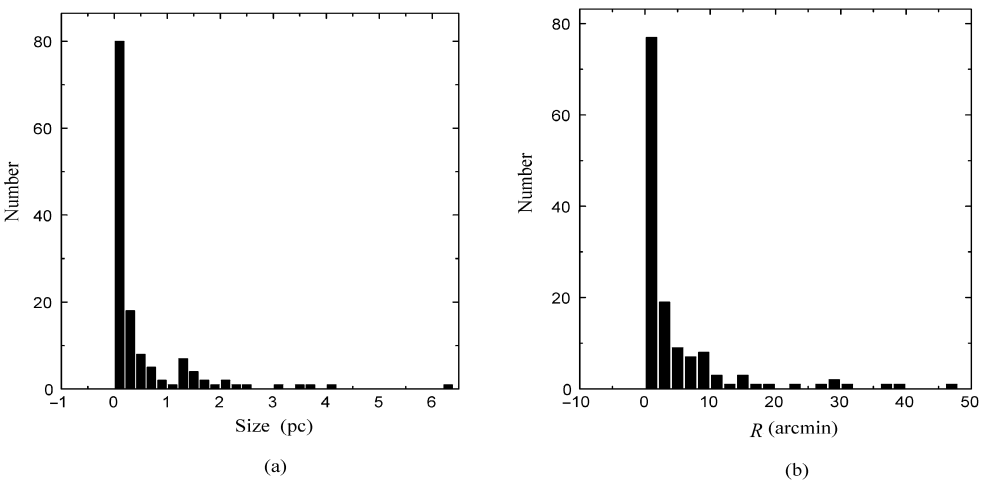

Fig. 1 (a) Number of HH objects at given distances (pc) from their energy sources;
(b) Number of HH objects at given apparent distances (arcmin) from their energy sources.

To investigate the difference between the IRAS energy sources and other nearby IRAS sources, we picked out all the IRAS sources that are within $10'$ of the HH object. There were 83 cases where other IRAS sources besides the one identified as the energy source of the HH object were found within the $10'$ area. In 57 (or 70%) of these 83 cases, the IRAS energy source is the brightest source (largest $L_{5-1000\mu\mathrm{m}}$); in 17 cases (or 20%), the HH energy source is the second brightest. These two groups make up 90% of the cases. This result shows that the HH energy source has a stronger infrared radiation than the other nearby "non-energy" sources.

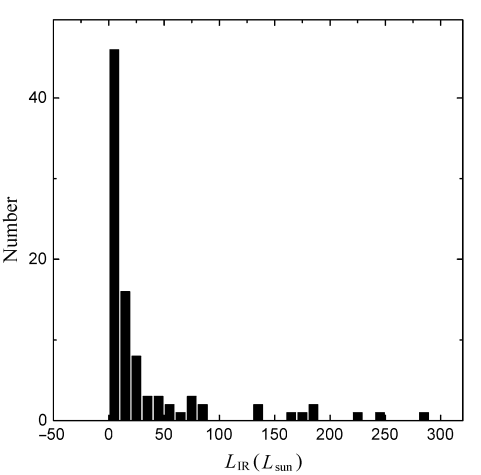

Fig. 2 Frequency distribution of IRAS luminosity of HH energy sources.

3.2 Color

Figures 3a and 3b are the IRAS color-color diagrams of the energy sources and nearby sources: Fig. 3a plots $\log\frac{f_{60}}{f_{25}}$ vs. $\log\frac{f_{25}}{f_{12}}$ and Fig. 3b plots $\log\frac{f_{100}}{f_{60}}$ vs. $\log\frac{f_{25}}{f_{12}}$. We can see from these two plots that the HH energy sources are concentrated in a band, and the nearby sources are not so concentrated.

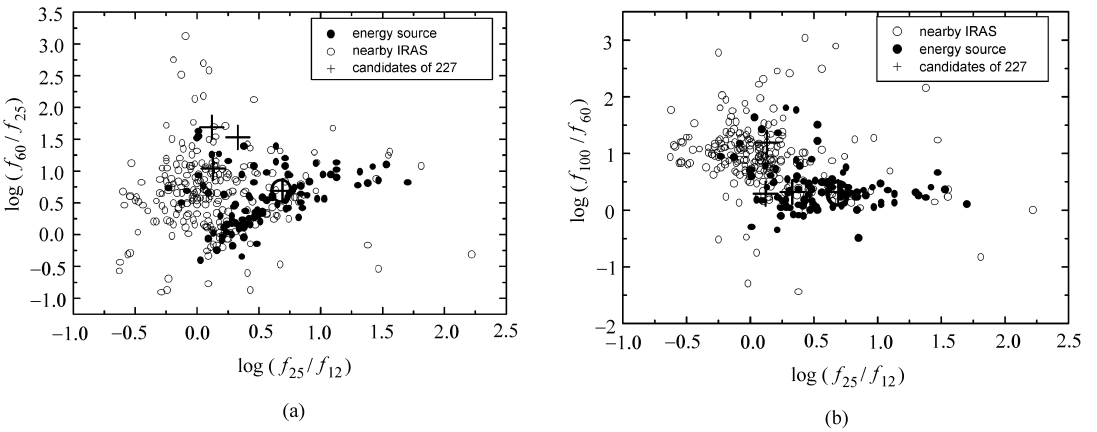

Fig. 3 IRAS color-color diagrams. Filled circles denote HH energy sources, empty circles denote nearby sources.

In Fig. 3b the band is almost parallel to the abscissa. This feature suggests that the rate of emission increase with increasing wavelength is faster in the shorter wavelengths than in the longer wavelengths. In the longer waveband, the energy sources have a similar color index close to 0.0. The difference may be due to the energy sources being deeply embedded in dusty material, which shields the radiation from the central star. Large dust grains are mainly silicates, they tend to exist in regions with a lower temperature than around a YSO. These large grains around the source have a strong infrared emission peaking at about 100 μm (Krügel & Walmsleg 1984). Thus, two consequences will be expected. First, the spectral energy distribution (SED) of these energy sources will reach a maximum at about 100 μm, so in the 60–100 μm range radiation will vary slowly here with a small slope in the SED curve, while the opposite will be the case for the 12–25 μm range. Also, when the surrounding material is thick enough, long wavelength emission is dominant and some uniform character in long wavelength flux can be expected for different energy sources. All these will lead to the band-shaped distribution in Fig. 3. Observations and theoretical analysis have already presented evidence for circumstellar envelopes and disks of Class I and II YSOs (Rucinsk 1985; Adams et al. 1988; Lada 1987). Second, such a thick envelope will have a strong infrared emission itself, resulting in a large observed infrared flux, which agrees well with the conclusion derived from Section 3.1 that the HH energy sources have large IRAS luminosities.

In an attempt to get more precise results, we removed all those IRAS energy sources that have one or more quality factors below 2. The remaining good-quality IRAS sources are replotted in Figs. 4a and 4b. Obviously, an even tighter distribution (marked out with straight lines) of the HH energy sources appears as we had hoped. The band-shaped region can now be expressed as:

From Fig. 4a: $0 < \log \frac{f_{25}}{f_{12}} < 1.6$, $1.1 \log \frac{f_{25}}{f_{12}} - 0.7 < \log \frac{f_{60}}{f_{25}} < 1.1 \log \frac{f_{25}}{f_{12}} + 0.2$ and from Fig. 4b as $0 < \log \frac{f_{25}}{f_{12}} < 1.6$, $-0.1 < \log \frac{f_{100}}{f_{60}} < 0.6$.

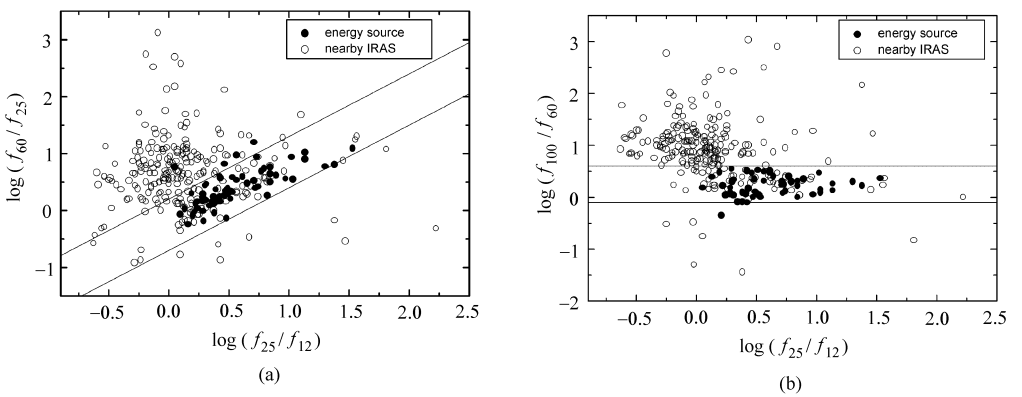

Fig. 4 As Fig. 3, but for good-quality sources only. Lines outline the region of concentration of HH energy sources.

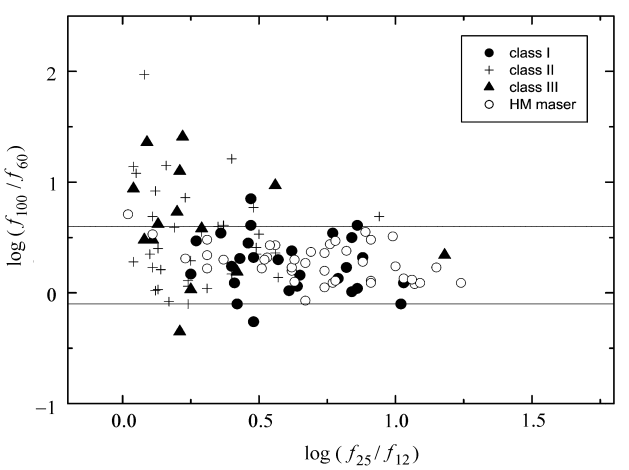

Fig. 5 Color-color diagram of class I, II, III sources and high-mass water maser sources.

4 SED ANALYSIS OF HH ENERGY SOURCES

Since the radiation flux of the HH energy sources varies slowly in the 60–100 μm range their SED there is flat, so their evolutionary status in the PMS period should be close to that of class I or class II sources. For this, we plot the color-color diagram for the group of class I, class II, and class III sources given by Chen et al. (1995) (Fig. 5). We find that nearly all the class I and part of the class II sources fall well inside the band, while class III sources do not. It can also be seen that the class I and class II sources are separated from one another at about $\log \frac{f_{25}}{f_{12}} = 0.4$. It is possible that with the surrounding material becomes thinner and weaker, the YSO moves from $\log \frac{f_{25}}{f_{12}} > 0.4$ region to the $0 < \log \frac{f_{25}}{f_{12}} < 0.4$ region. As the circumstellar material is dispersed, the position of the YSOs in the diagram will be dispersed, too. The fact

that the band-shaped distribution has a definite beginning and ending suggests that HH objects can only happen during a certain phase corresponding to a certain range in the thickness of the surrounding material.

To test the effect of mass on the band-shaped distribution, we put a group of high-mass H_2O maser sources ($L_{\rm bol} > 5000\,L_\odot$) given by Wu et al. (2001) on diagram (see Fig. 5). They also fit well into the band. Moreover, it seems that these sources fall quite close to the class I sources. This suggests that the band-shaped distribution is rather sensitive to evolutionary age. Its appearance tells the fact that the sources in the region are very young.

5 IDENTIFICATION OF HH ENERGY SOURCES

The statistical result shows that the energy sources of HH objects are class I or class II YSOs. Comparing with other IRAS sources, the IRAS HH energy sources have a larger IRAS luminosity and are located in a particular band-shaped region in the color-color diagram. With these characteristics, we can now try to identify the energy sources for those HH objects whose energy sources are yet unknown. First, we picked out 13 HH objects whose energy sources have been suggested by other methods but not been confirmed in the General Catalogue (Repurth 1999), they are HH 132, 192, 197, 212, 224, 227, 251, 281, 290, 360, 392, 422, and 427. They all have more than one nearby IRAS sources. Taking HH 227 as example, there are four IRAS sources within $10'$ of HH 227; we put all four on the color-color diagrams (see Figs. 3a and 3b). We find that IRAS 06571–0441 falls in the band-shaped energy source region in the two diagrams. It also has the greatest IRAS luminosity among the four sources. And the other three fall outside the band-shaped region. So we take IRAS 06571–0441 (marked by a cross with a circle outside in Fig. 3) as the candidate IRAS energy source for HH 227. In this way, we identified the energy source candidates for the 13 HH objects. On comparing our results with the suggested sources in the General Catalogue we find agreement in all cases except in case of HH 422.

Then we applied this method to more than 200 remaining HH objects without known energy sources. The results are listed in Table 1. Column 1 (and 5) names the HH object, column 2 (and 6) and 3 (and 7) give the position (B1950). Column 4 (and 8) names the identified energy source. Some HH objects have no nearby IRAS sources nearby; —these are marked "n". In some cases we find none of the nearby IRAS sources qualified as the energy source candidate and that the driver of the HH object may be some other infrared or radio sources around; —these cases are marked "m". Cases where the present method is ineffective are marked with "c". Finally, we have 96 HH objects whose energy sources are identified by the present method.

6 THE DISTRIBUTION OF EARLY-STAGE YSOs IN THE GALAXY

The sources located in the band-shaped region of the color-color diagrams have rather red color indices and large IRAS luminosities and are closely associated with HH objects. These are very important characters of early-aged YSOs. We utilize these characters to pick out candidates of early-stage YSOs which need further study for their evolutionary status. Our criteria are: 1) colors: we confine to the band region in the color-color diagrams as specified at the end of Section 3.1; 2) the quality index Q, we restrict $Q \geq 2$; 3) galactic latitude, we only accept the candidates whose galactic latitude are between $+25^\circ$ and -25° for excluding infrared galaxies. We pick out a group of candidates from IRAS PSC according to the criterion above.

Table 1 Identification of Energy Sources of HH Objects

HH No.	RA (1950)	DEC (1950)	Energy Source	HH No.	RA (1950)	DEC (1950)	Energy Source
280	3 20 40.5	+ 30 07 22	n	14	3 25 44.4	+ 30 50 56	03254+3050
267	3 20 58.3	+ 30 49 53	n	341	3 25 44.8	+ 30 59 16	c
268	3 21 17.6	+ 30 37 36	n	334	3 25 46.0	+ 31 12 19	03260+3111
193	3 21 48.1	+ 30 44 22	03225+3034	342	3 25 46.5	+ 31 00 29	c
194	3 21 54.1	+ 30 37 09	03225+3034	343	3 25 49.1	+ 30 55 02	03254+3050
196	3 22 08.9	+ 30 38 46	03225+3034	426	3 25 49.3	+ 30 42 07	n
195	3 22 10.4	+ 30 36 28	03225+3034	350	3 25 49.6	+ 30 54 22	03254+3050
197	3 22 32.3	+ 30 34 32	03225+3034	15	3 25 53.5	+ 30 57 43	03255+3103
277	3 23 00.1	+ 30 28 51	n	344	3 25 56.2	+ 31 02 57	03259+3105
278	3 23 55.1	+ 30 15 32	n	16	3 26 02.8	+ 30 58 52	c
317	3 24 07.3	+ 30 01 34	n	333	3 26 06.1	+ 31 15 51	c
279	3 24 14.5	+ 30 06 51	03245+3002	345	3 26 09.6	+ 31 03 08	03259+3105
423	3 24 30.9	+ 30 05 30	03245+3002	6	3 26 07.0	+ 31 08 23	03259+3105
318	3 24 40.5	+ 30 03 54	03245+3002	347	3 26 10.2	+ 31 05 04	03259+3105
422	3 24 43.9	+ 30 01 15	03245+3002	335	3 26 12.0	+ 31 12 45	c
338	3 25 07.3	+ 31 09 22	03255+3103	352	3 26 13.1	+ 30 49 46	n
351	3 25 13.0	+ 30 40 09	n	17	3 26 14.7	+ 31 08 17	m
339	3 25 25.5	+ 31 04 25	03255+3103	5	3 26 14.8	+ 31 02 34	03259+3105
340	3 25 39.7	+ 30 55 19	03254+3050	4	3 26 18.6	+ 31 09 41	03260+3111
13	3 25 42.1	+ 30 56 47	03254+3050	348	3 26 19.9	+ 31 03 17	m
18	3 26 21.0	+ 30 57 21	n	393	4 27 48.6	+ 24 34 59	04278+2435
336	3 26 30.1	+ 31 09 08	m	265	4 28 21.0	+ 18 05 35	n
349	3 26 30.7	+ 31 03 16	m	264	4 28 24.6	+ 17 59 52	04287+1801
353	3 26 32.2	+ 31 19 56	m	263	4 28 29.5	+ 18 01 24	04287+1801
368	3 27 19.2	+ 30 20 43	03271+3013	266	4 28 58.2	+ 18 10 28	c
369	3 27 22.3	+ 30 18 11	03271+3013	319	4 29 39.4	+ 24 15 27	c
370	3 27 28.3	+ 30 17 31	03271+3013	286	4 29 47.6	+ 18 10 18	n
427	3 27 33.1	+ 30 11 43	n	467	4 30 31.2	+ 24 14 12	04305+2414
371	3 27 41.2	+ 30 20 45	03276+3022	468	4 30 35.9	+ 24 15 28	04305+2414
372	3 27 41.2	+ 30 19 13	03276+3022	192	4 36 43.4	+ 25 57 37	c
428	3 27 42.4	+ 30 27 51	n	328	5 15 13.4	+ 07 12 47	m
429	3 28 42.4	+ 30 59 50	n	329	5 15 58.6	+ 07 05 12	m
430	3 29 21.7	+ 31 14 32	n	190	5 27 27.5	+ 33 45 38	05274+3345
356	3 29 59.8	+ 31 16 39	n	58	5 28 22.7	− 04 11 44	05283-0412
211	3 40 48.2	+ 31 51 28	c	59	5 29 52.0	− 06 31 09	n
362	4 01 20.5	+ 26 12 31	04106+2610	60	5 30 11.4	− 06 28 50	n
361	4 01 32.4	+ 26 13 35	04106+2610	131	5 32 18.9	− 08 30 03	n
360	4 01 40.5	+ 26 10 51	04106+2610	331	5 32 40.4	− 05 02 42	m
392	4 17 49.8	+ 26 52 46	c	269	5 32 41.7	− 05 25 38	m
276	4 19 02.8	+ 26 50 25	04189+2650	201	5 32 44.0	− 05 23 48	c
202	5 32 44.0	− 05 24 40	c	173	5 33 08.7	− 06 34 53	m
205	5 32 44.4	− 05 22 18	05330–0517	134	5 33 10.1	− 06 32 10	05329–0628
206	5 32 45.0	− 05 22 32	05330–0517	324	5 33 14.0	− 06 20 25	c
207	5 32 45.2	− 05 22 43	05330–0517	330	5 33 14.2	− 05 06 34	c
208	5 32 46.3	− 05 24 15	n	310	5 33 22.2	− 05 37 56	m
209	5 32 46.4	− 05 23 40	n	326	5 33 23.2	− 06 33 55	m
323	5 32 46.5	− 06 19 35	m	127	5 33 24.4	− 07 02 08	n
322	5 32 46.8	− 06 21 45	m	325	5 33 24.5	− 06 31 10	n
210	5 32 48.0	− 05 22 34	c	327	5 33 24.6	− 06 37 20	m

Table 1 Continued

HH No.	RA (1950)	DEC (1950)	Energy Source	HH No.	RA (1950)	DEC (1950)	Energy Source
357	5 32 48.3	– 05 08 03	m	316	5 33 28.1	– 06 06 44	n
44	5 32 48.5	– 05 12 19	m	308	5 33 34.4	– 06 02 15	n
407	5 32 50.5	– 06 01 32	m	309	5 33 36.2	– 05 51 37	n
293	5 32 53.6	– 05 03 08	c	307	5 33 41.0	– 06 06 05	c
203	5 32 54.8	– 05 26 51	m	306	5 33 41.5	– 06 10 36	c
385	5 32 55.0	– 05 09 13	m	299	5 33 43.3	– 06 21 49	05338–0624
204	5 32 55.2	– 05 27 06	m	296	5 33 45.2	– 06 19 12	05338–0624
384	5 32 57.7	– 05 11 16	m	3	5 33 45.8	– 06 44 53	05339–0646
383	5 32 58.7	– 05 09 45	m	61	5 33 47.4	– 07 08 51	n
287	5 33 01.9	– 05 07 08	c	62	5 33 47.5	– 07 12 51	n
45	5 33 06.3	– 04 52 43	c	145	5 33 48.5	– 06 48 11	05339–0646
297	5 33 49.3	– 06 18 22	c	64	5 35 22.3	– 07 07 12	m
298	5 33 55.4	– 06 23 40	05338–0624	38	5 35 56.5	– 07 13 18	05357–0710
146	5 33 56.8	– 06 50 10	05339–0646	446	5 36 54.9	– 02 35 05	c
305	5 33 57.0	– 06 17 32	m	66	5 37 55.0	– 02 04 04	c
148	5 33 57.4	– 06 45 03	05339–0646	67	5 38 32.6	– 01 48 06	c
304	5 34 10.6	– 06 16 42	m	68	5 39 8.7	– 06 27 20	c
301	5 34 12.7	– 06 23 04	05338–0646	69	5 39 15.6	– 06 31 18	c
36	5 34 20.7	– 06 46 01	c	92	5 39 48.9	– 01 19 52	c
63	5 34 21.0	– 04 27 45	c	93	5 40 23.8	– 01 27 08	c
302	5 34 22.0	– 06 22 25	c	94	5 40 56.3	– 02 34 14	n
285	5 34 30.5	+ 31 57 17	05345+5157	212	5 41 18.9	– 01 04 09	05413–0104
281	5 34 32.8	+ 31 58 28	05345+5157	95	5 41 22.5	– 02 39 03	n
282	5 34 33.5	+ 31 58 19	05345+5157	19	5 43 16.0	– 00 06 20	n
283	5 34 34.8	+ 31 58 11	05345+5157	20	5 43 21.5	– 00 04 14	m
403	5 34 36.7	– 05 54 40	n	21	5 43 22.0	– 00 05 36	n
284	5 34 38.3	+ 31 57 51	05345+5157	37	5 43 22.2	– 00 06 39	05435–0011
404	5 34 48.7	– 05 45 49	m	70	5 43 28.7	– 00 06 43	05435–0011
405	5 34 57.7	– 05 45 20	c	22	5 43 40.3	– 00 06 36	05435–0011
406	5 35 11.7	– 05 41 05	c	27	5 43 49.4	– 00 14 45	05435–0011
89	5 35 21.9	– 06 47 47	c	291	5 44 02.9	+ 20 58 48	05440+2059
290	5 44 04.5	+ 20 59 08	05440+2059	136	11 10 09.0	– 58 29 44	11101–5829
71	5 44 46.1	+ 00 39 43	m	137	11 11 49.0	– 60 36 17	m
110	5 48 47.8	+ 02 54 09	05487+0255	138	11 12 01.5	– 60 36 35	m
112	5 49 14.4	+ 02 59 47	05489+0256	320	11 58 58.8	– 64 51 29	11590–6452
122	5 52 03.2	+ 01 43 26	c	77	14 56 42.9	– 62 55 53	14564–6254
273	6 10 18.3	– 06 10 56	06103–0612	141	14 59 14.9	– 63 12 09	14592–6311
272	6 10 21.9	– 06 10 30	06103–0612	142	14 59 17.6	– 63 10 41	14592–6311
226	6 38 17.2	+ 09 42 42	m	143	14 59 19.6	– 63 11 51	14592–6311
225	6 38 17.7	+ 09 47 09	m	187	15 42 07.2	– 34 08 11	15420–3408
125	6 38 20.3	+ 09 50 28	m	78	16 05 51.3	– 38 57 10	m
227	6 57 07.9	– 04 41 58	06571–0441	418	16 23 11.8	– 24 34 15	c
246	8 19 45.7	– 49 29 59	c	419	16 23 22.9	– 24 24 06	16231–2427
132	8 33 40.4	– 40 28 28	08337–4028	314	16 23 37.2	– 24 34 10	16239–2428
73	9 00 26.6	– 44 39 25	n	79	16 23 45.1	– 24 13 42	16235–2416
74	9 00 28.6	– 44 37 59	n	224	16 24 15.0	– 24 40 31	m
133	9 09 02.4	– 45 18 18	m	416	16 24 41.2	– 24 42 39	m
75	9 09 50.7	– 45 30 07	c	417	16 25 24.4	– 24 21 25	m
171	9 46 59.2	– 54 43 05	m	420	16 25 36.5	– 24 30 34	m
51	11 08 21.5	– 76 08 01	n	213	17 59 26.6	– 24 17 16	n

Table 1 Continued

HH No.	RA (1950)	DEC (1950)	Energy Source	HH No.	RA (1950)	DEC (1950)	Energy Source
135	11 10 05.9	− 58 30 14	11101–5829	399	17 59 26.7	− 23 04 04	m
180	18 14 25.2	− 19 52 55	m	242	21 41 29.9	+ 65 52 50	m
216	18 16 05.1	− 13 53 03	n	238	21 41 31.4	+ 65 51 55	21418+6552
476	18 26 26.3	+ 00 27 12	18265+0028	237	21 41 33.3	+ 65 51 37	21418+6552
477	18 27 06.2	+ 01 18 20	m	239	21 41 35.2	+ 65 52 51	21418+6552
460	18 27 06.4	+ 01 16 20	m	236	21 41 50.2	+ 65 53 52	21418+6552
478	18 27 24.2	+ 01 13 35	m	105	21 42 12.9	+ 65 54 00	21418+6552
456	18 27 26.9	+ 01 09 10	m	234	21 42 20.6	+ 65 54 50	m
457	18 27 27.6	+ 01 08 41	m	235	21 42 33.5	+ 65 54 38	m
172	18 51 32.7	+ 0 28 52	m	251	22 17 57.4	+ 63 17 50	22178+6317
332	19 18 05.3	+ 10 54 58	c	252	22 18 01.1	+ 63 17 32	22178+6317
475	20 22 53.9	+ 42 05 40	c	253	22 18 08.4	+ 63 16 38	22178+6317
166	20 27 36.0	+ 40 01 16	n	254	22 18 12.7	+ 63 16 09	22178+6317
415	20 45 34.2	+ 67 49 25	20453+6746	373	22 35 55.9	+ 74 59 40	n
382	20 56 52.3	+ 52 05 39	20568+5217	374	22 36 33.6	+ 74 51 54	n
380	20 57 39.7	+ 52 22 31	20568+5217	364	22 37 13.5	+ 74 57 29	n
198	21 00 24.0	+ 78 11 00	21004+7811	358	23 22 42.2	+ 73 56 06	n
103	21 41 15.8	+ 65 49 55	n	359	23 24 30.7	+ 74 05 57	n
232	21 41 18.0	+ 65 50 42	n				

Notes to Table 1: n: no IRAS sources nearby; m: the energy source may not be a nearby IRAS source; c: cannot be judged by the present method.

The selected YSO candidates are shown in galactic coordinates over a background of the Columbia CO Sky Survey (Dame et al. 1987). They are compared with the distribution of HH objects and another typical star formation indicator, molecular outflows (Wu et al. 1996) in the vicinity of the Galactic Equator (see Fig. 6).

Figure 6 shows that the early-stage YSO candidates are closely associated with HH objects and outflows. In some famous star formation regions like Taurus, Orion and Perseus, the candidates are concentrated. In other regions where HH objects or outflows data are not available, the concentrated appearance of YSO candidates suggest that large scale star formation may be proceeding in these regions. It is worth searching for new HH objects or molecular outflows in such regions.

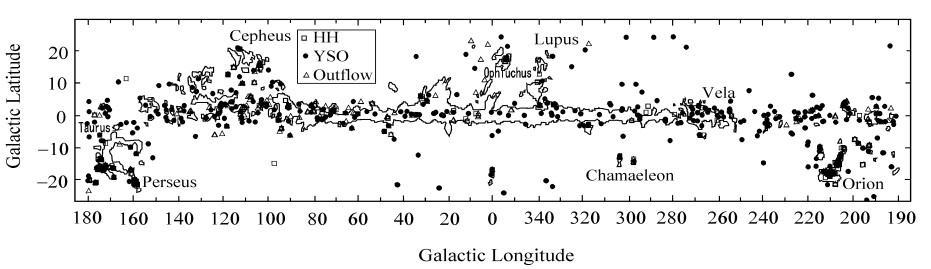

Fig. 6 Distribution of early-stage YSOs in the vicinity of the Galactic Equator. Contours are Columbia CO sky survey results from Dame et al. (1987).

7 SUMMARY

The major conclusions we draw in this paper are as follows:

1) The majority of energy sources of HH objects have IRAS counterparts. They usually have a greater IRAS luminosities and are younger than other nearby IRAS sources.

2) HH objects are commonly located within 0.5 pc of their energy sources, and the peak of distribution is within 0.2 pc. However, some of them could be as far as several pc; in angular distance, most of them are within 10 arcmin of their sources. About 80% of the IRAS energy sources have an IRAS luminosity less than $50\,L_{\odot}$, which suggests that the energy sources of HH objects are chiefly low-mass sources.

3) The energy sources of HH objects appear in a particular band-shaped region in IRAS color-color diagrams. Using this color characters and combining with luminosity data we have identified the energy sources of hitherto unidentified HH objects.

4) The energy sources of HH objects are class I or class II type young stars which are wrapped inside thick circumstellar material. The band-shaped distribution in color-color diagram is evidence of this surrounding material. We use this color property to pick out early-stage young stellar objects which have similar characters to HH energy sources to trace the large scale star forming activities. Besides, a group of YSO candidates are picked out and plotted on the CO distribution of Columbia Sky Survey, together with HH objects and outflows. These sources are worthy of further study.

Acknowledgements We are grateful to the helpful discussion of participants of the star formation workshop organized by CAS-PKU Joint Beijing Astrophysics Center in May 1999. We thank Sun Jin, Wang Junjie, Yao Yongqiang, Yang Ji and Zhao Bing for their stimulating conversations. This project is supported by G1999075405 of NKBRSF, 19773002 of the NSFC.

References

Adams F., Lada C., Shu F., 1988, ApJ, 326, 865
Bome K. -H., 1956, ApJ, 123, 379
Casoli F., Dupraz C., Gerin M. et al., 1986, A&A, 169, 281
Chen H., Myers P. C., Ladd E. F. et al., 1995, ApJ, 445, 377
Dame M., Ungerechts H., Cohen R. S. et al., 1987, ApJ, 332, 706
Emerson J. P., 1987, In: M. Pembert, J. Jugaku, eds., IAU Symp. 115, Star Formaing Regions, Dordrecht: Reidel, p.19
Gezari D. Y., Pitts P. S., Schmitz M. et al., 1996, Calalog of Infrared Observations, Edition 3.5
Herbig G. H., 1951, ApJ, 113, 697
Hoyle F., 1956, ApJ, 124, 484
Krügel E., Walmsleg C. M., 1984, A&A, 130, 5
Lada C., 1987. In: M. Pembert, J. Jugaku, eds., Star Formation Regions, Boston: Reidel, p.1
Reipurth B., In: B. Reipurth, C. Bertout, eds., IAU Symp. 182, Herbig-Haro Flows and the Birth of Low Mass Stars, 1997, p.3
Reipurth B., 1999, A General Catalogue of Herbig-Haro Objects, 2. Edition (http://casa.colorado.edu/hhcat)
Rucinski S., 1985, AJ, 90, 2321
Weintraub D. A., 1990, ApJS, 74, 575
Wu Y., Huang M., He J., 1996, A&AS, 115, 283
Wu Y., Yang C., Li Y., 2001, preprint